

***Ab initio* and analytical studies of the spin-orbit coupling in heteronuclear alkali-metal dimers AB (A, B = Li, Na, K, Rb) at long ranges**

E. A. Bormotova, S. V. Kozlov, E. A. Pazyuk, and A. V. Stolýarov\*

*Department of Chemistry, Lomonosov Moscow State University, 119991 Moscow, Leninskie gory 1/3, Russia*

W. Skomorowski

*Department of Chemistry, University of Southern California, Los Angeles, California 90089, USA*

I. Majewska and R. Moszynski†

*Quantum Chemistry Laboratory, Department of Chemistry, University of Warsaw, Pasteura 1, 02-093 Warsaw, Poland*

(Received 10 November 2018; published 11 January 2019)

The spin-orbit (SO) coupling matrix elements between the excited states of the lightest heteronuclear alkali metal dimers AB (A, B = Li, Na, K, Rb) converging to the first three dissociation limits were evaluated by employing the quasirelativistic electronic wave functions in a wide range of interatomic distances,  $R$ . The inner-shell electrons of alkali atoms were described using nonempirical shape-consistent effective core potentials. To take the core-valence correlation effects into account, core polarization potentials for each atom were implemented. Dynamical correlation was introduced through the multireference configuration interaction method, which was applied to two valence electrons keeping all subvalence electrons frozen. The reliability of the derived SO functions is accessed through comparison, wherever possible, with their preceding theoretical and experimental counterparts. The *ab initio* SO matrix elements were approximated beyond the LeRoy radius using the formula:  $\xi_{if}^{SO}(R) = \alpha + \beta_{if}^{[k]}/R^k$ , where (1)  $k = 6$  and  $\alpha = \xi_{n^2P}^{SO}$  is the SO splitting of the atom  $A(n^2P)$  for the states of the AB molecule converging to the same  $A(n_A^2P) + B(n_B^2S)$  dissociation limit, and (2)  $k = 3$  and  $\alpha = 0$  for the molecular  $i$  and  $f$  states converging to the  $A(n_A^2P) + B(n_B^2S)$  and  $A(n_A^2S) + B(n_B^2P)$  atomic thresholds, respectively. A theoretical justification of these formulas was derived from the multipole expansion of the molecular SO operator in terms of the inverse powers of the internuclear distance and of products of operators acting on the electronic coordinates of the atoms A and B.

DOI: [10.1103/PhysRevA.99.012507](https://doi.org/10.1103/PhysRevA.99.012507)**I. INTRODUCTION**

The spin-orbit (SO) coupling effect is the main source of intramolecular perturbations due to the flexible selection rules for the corresponding SO operator [1]. Typically, the strength of the SO interaction decreases as electronic excitation increases. However, the impact of this interaction on the nonadiabatic mixing of excited states does not diminish, instead remaining significant, because the density of interacting states grows rapidly when looking at more highly excited states. The SO functions themselves, expectedly, are strongly dependent on internuclear distance,  $R$ , and their long-range tails are responsible for the complex dynamics of states near the dissociation threshold. Therefore, a rigorous coupled-channel (CC) deperturbation treatment [2] of the excited diatomic states with spectroscopic (experimental) accuracy indispensably includes detailed potential energy curves (PECs) and SO functions over a wide range of internuclear distances.

This requirement is furthermore complicated by the fact that the optical pathways most frequently applied in

photoassociation [3], magnetoassociation [4], and stimulated Raman adiabatic passage [5] (STIRAP) processes of ultracold atom assembly [6,7] include bound and quasi-bound rovibronic levels located in the vicinity of the dissociation threshold. Therefore, it is necessary that both PEC and SO functions be *physically* correct over the entire range of  $R$ , so the relevant Feshbach resonances can be predicted with the required spectroscopic accuracy.

The SO coupling effect is especially dominant in the complex electronic structure of open-shell diatomic systems (in particular, those containing a transition metal) which are important in the astrophysics of “cool” stars, brown dwarfs, and, most recently, extrasolar planets [8]. In addition, the SO interaction dramatically changes the radiative, magnetic, and electric properties of the excited molecular states. The pronounced SO coupling makes intercombination (spin-forbidden) transitions, autoionization, and dissociative recombination possible and plays a crucial role in the correct description of the collisions of slow atoms in cold plasma.

The adiabatic interatomic potentials for the ground and low-lying excited electronic states of homonuclear and heteronuclear [9] alkali dimers were comprehensively studied (both experimentally and theoretically) during the past three decades [10]. The corresponding quasirelativistic and fully relativistic PECs of K-, Rb-, and Cs-containing molecules

\*avstol@phys.chem.msu.ru

†rmoszyns@tiger.chem.uw.edu.pl

[11–15] were also evaluated using *ab initio* methods. However, the electronic SO coupling functions,  $\xi_{if}^{SO}(R)$ , needed for a robust CC deperturbation analysis in explicit form, are known, at present, for a very limited number of both homonuclear [16] and heteronuclear [17] alkali diatomic states. Indeed, the most extensive *ab initio* calculations of reliable SO matrix elements were performed for the NaK [18–21] and NaRb [22,23] molecules. Highly accurate SO matrix elements were extracted in the course of a CC deperturbation treatment of the low-lying singlet-triplet  $A(1)^1\Sigma^+ \sim b(1)^3\Pi$  complexes of NaK [21], NaRb [22,23], and KRb [24]. In the case of NaK, the more highly excited singlet-triplet  $B(1)^1\Pi \sim c(2)^3\Sigma^+$  and  $D(2)^1\Pi \sim d(2)^3\Pi$  complexes were additionally investigated [18,19,25]. Contrary to their theoretical counterparts, the resulting empirical SO matrix elements are determined in a very narrow interval of  $R$ . The *ab initio* SO matrix elements for Li-containing dimers are still not available (except for a few matrix elements calculated for the LiCs molecule [26]), even though a pronounced SO coupling effect was recently discovered in the photoassociation spectra of the LiRb molecule [27,28].

Long-range perturbation theory [29–33] has been well established for the asymptotic construction of PECs, electric properties, and electronic transition dipole moment functions (ETDMs) [34–37] at large internuclear distances. Recently, the long-range behavior of the *ab initio* calculated ETDMs functions was numerically studied for homonuclear [38]  $A_2$  ( $A = \text{Rb}, \text{Cs}$ ) and heteronuclear [39] dimers  $AB$  ( $A, B = \text{Li}, \text{Na}, \text{K}, \text{Rb}$ ), while, to the best of our knowledge, no long-range study was reported for the corresponding SO functions.

Therefore, the present paper aims to fill this gap focusing on systematic *ab initio* calculations of the SO coupling matrix elements between the low-lying states of the lightest heteronuclear alkali metal dimers over a wide range of  $R$  conducting both analytical and numerical long-range analysis beyond the modified LeRoy radius [40]. Additionally, a multipole expansion of the molecular SO operator in terms of the inverse powers of  $R$ , and products of operators acting on the electronic coordinates of the atoms A and B will be introduced to analytically explain the long-range behavior of the computed SO coupling matrix elements.

Fitting high-resolution spectra to extract accurate empirical potential energy curves and nonadiabatic couplings represents a formidable task, and Professor Robert J. LeRoy was one of the pioneers in this field. In a series of computer programs [41–45], LeRoy developed open-ended tools to perform direct-potential-fits (DPFs) with physically reliable analytic forms. See, for instance, Refs. [46–55] for various applications of these inversion procedures to alkali metal dimers. It is worth noting that the approach to fitting the potentials in the long range introduced by LeRoy [56] was used, among others, to discriminate between different *ab initio* and empirical long-range coefficients [57–59].

## II. AB INITIO CALCULATIONS OF THE SPIN-ORBIT MATRIX ELEMENTS

We obtained the electronic wave functions  $\psi_i^{ab} \equiv |S, \Sigma, \Lambda(\Omega = \Lambda + \Sigma)\rangle$  for the lightest heteronuclear alkali metal dimers  $AB$  ( $A, B = \text{Li}, \text{Na}, \text{K}, \text{Rb}$ ) within the framework

TABLE I. Static electric dipole polarizabilities of the cation [66],  $\alpha_c^+$ , and the exponential cutoff parameters,  $k_c$ , used to build the core-polarization potentials (CPPs) for the Li, Na, K, and Rb atoms with the principal quantum numbers  $n = 2, 3, 4$ , and 5, respectively. The  $\alpha_c^+$  and  $k_c$  values are given in a.u., while the relevant atomic nonrelativistic energies,  $\omega$ , and spin-orbit splitting parameters,  $\xi_{n^2P}^{SO}$ , are in  $\text{cm}^{-1}$ .

	$\alpha_c^+$	$k_c$	$\omega(n^2S - n^2P)$		$\xi_{n^2P}^{SO}$	
			exp	calc	exp	calc
Li	0.1997	2.42 <sup>a</sup>	14 903	14 903	0.335	0.315
Na	0.9947	0.65 <sup>a</sup>	16 967	16 947	17.196	17.224
K	5.354	0.247 <sup>a</sup>	13 023	13 013	57.710	57.688
Rb	9.096	0.379 <sup>b</sup>	12 737	12 705	237.595	237.731

<sup>a</sup>Stoll-Fuentealba damping function.

<sup>b</sup>Mueller-Meyer damping function.

of quasirelativistic (scalar) electronic structure calculations corresponding to Hund's coupling case (a). According to the selection rule  $\Delta\Omega = 0$  in the pure Hund's coupling case (c), both singlet-triplet  $^1\Sigma^+ - ^3\Pi$ ,  $^1\Pi - ^3\Sigma^+$ ,  $^1\Pi - ^3\Pi$  and triplet-triplet  $^3\Pi - ^3\Sigma^+$ ,  $^3\Pi - ^3\Pi$  spin-orbit (SO) coupling matrix elements  $\xi_{if}^{SO}(R) = \langle \psi_i^{ab} | H_{SO} | \psi_f^{ab} \rangle$  between the individual quasirelativistic eigenstates were evaluated using the corresponding spin-orbit parts of the atomic pseudopotentials. All stages of the electronic structure calculations were carried out with the MOLPRO package [60]. The computational protocol used in the present work is described elsewhere [12,39] in detail.

Briefly, the inner core shells of the Li, Na, K, and Rb atoms were replaced by shape-consistent nonempirical effective core potentials [61] (ECP), leaving one valence electron of the Li and Na atoms and nine outer shell (eight subvalence plus one valence) electrons of the K and Rb atoms for explicit treatment. The Hartree-Fock molecular orbitals were optimized as solutions of the state-averaged complete active space self-consistent field (SA-CASSCF) problem performed for 2 (LiNa), 10 (LiK, LiRb, NaK, NaRb), and 18 (KRb) electrons on the  $(1-8)^{1,3}\Sigma^+$ ,  $(1-5)^{1,3}\Pi$ , and  $(1, 2)^{1,3}\Delta$  electronic states taken with equal weights [62]. The dynamical correlation was introduced via the internally contracted multireference configuration interaction (MRCI) method [63], which was applied to two valence electrons keeping all subvalence electrons frozen,

TABLE II. The sign-consistent multiplicative factors [68] of the spin-orbit electronic matrix elements,  $\xi_{if}^{SO}$ , calculated using *ab initio* methods for alkali metal AB dimers at  $R \rightarrow +\infty$ .

Transition	factor
$^3\Pi_{0^\pm} - ^3\Pi_{0^\pm}$	+1
$^3\Pi_{1-3}\Pi_1$	+1
$^3\Pi_{2-3}\Pi_2$	+1
$^3\Pi_{1-1}\Pi_1$	-1
$^3\Pi_{1-3}\Sigma_1^+$	+1
$^1\Pi_{1-3}\Sigma_1^+$	+1
$^3\Pi_{0^+-1}\Sigma_{0^+}$	$-\sqrt{2}$
$^3\Pi_{0^--3}\Sigma_{0^-}$	$+\sqrt{2}$

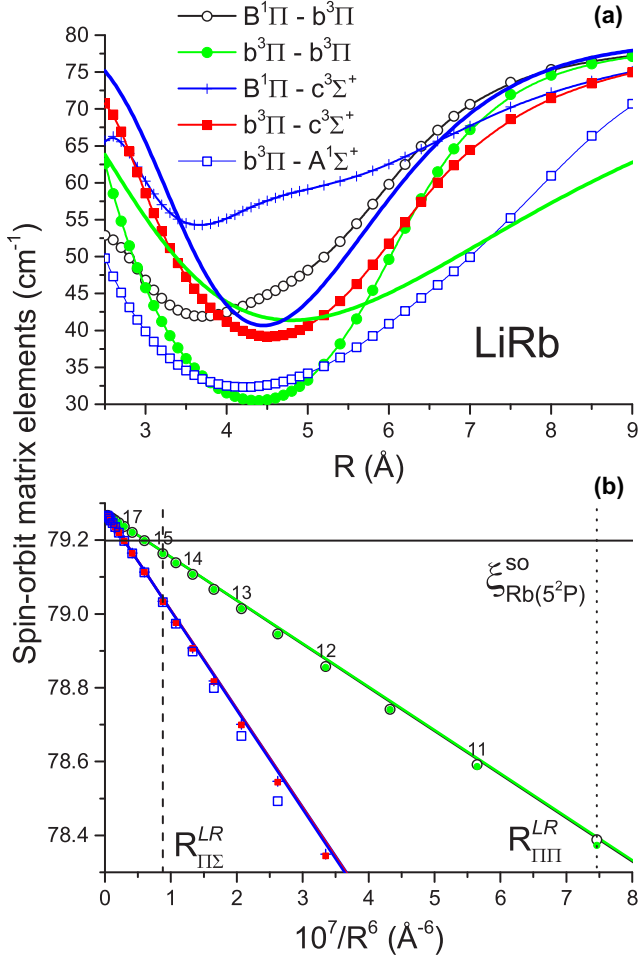


FIG. 1. (a) The present *ab initio* spin-orbit matrix elements between electronic states of LiRb converging to the second Li(2<sup>2</sup>S) + Rb(5<sup>2</sup>P) dissociation limit. The solid lines indicate SO matrix elements estimated in Ref. [17]; (b) the asymptotic behavior of the present  $\xi_{ij}^{SO}$  values with respect to the  $1/R^6$  coordinate.

i.e., 2 electrons in the case of LiNa, 8 electrons for LiK, LiRb, NaK, and NaRb, and 16 electrons for KRb.

We employed *l*-independent core polarization potentials (CPPs) [64] to take the core polarization effect into account. Both Stoll-Fuentealba [65] and Mueller-Meyer [64] damping functions were implemented within the present CPP construction. The required static dipole polarizabilities of the atomic core,  $\alpha_c^+$  (i.e., of the singly charged atomic cation) were taken from Ref. [66]. The initial sets of the exponential cutoff parameter,  $k_c$ , were adjusted to reproduce the experimental spin-averaged atomic energies (estimated at the center of gravity of the alkali doublets according to the Landé rule) for the lowest excited  $n^2P$  atomic states:  $\omega(n^2S - n^2P) = E(n^2P_{3/2}) - \xi_{n^2P}^{SO}/3$ . The atomic SO splitting parameters  $\xi_{n^2P}^{SO} = E(n^2P_{3/2}) - E(n^2P_{1/2})$  were estimated from the experimental termvalues of the corresponding  $n^2P$  doublets [67]. The resulting  $\alpha_c^+$  and  $k_c$  parameters applied to construct the present CPPs of the Li, Na, K, and Rb atoms are given in Table I.

It should be noted that the sign of the originally calculated SO matrix elements is not well defined since the phase of the corresponding electronic wave functions is arbitrary during

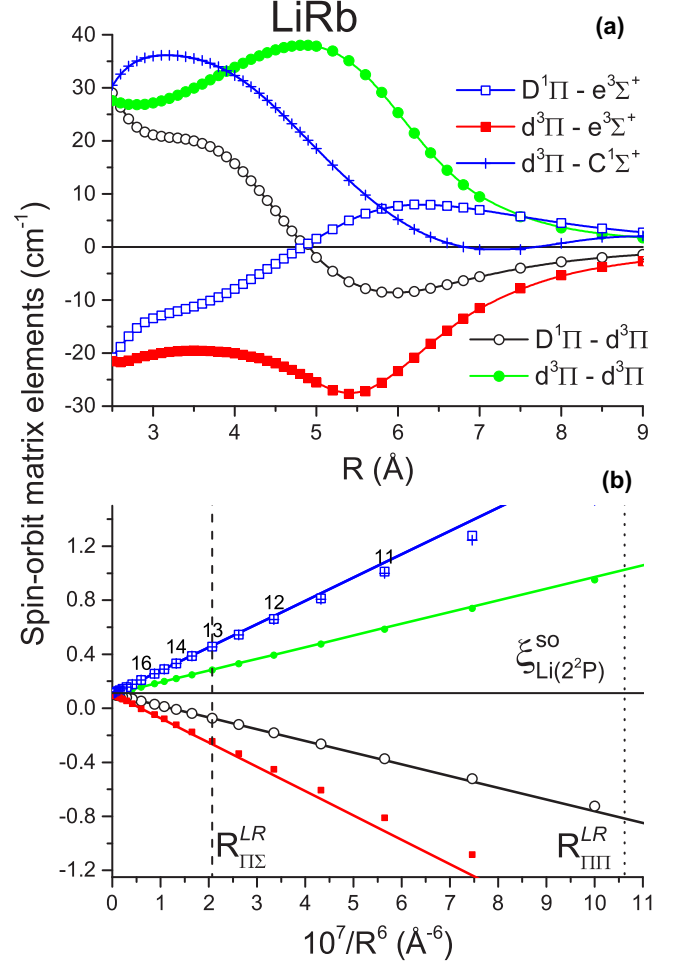


FIG. 2. (a) The present *ab initio* spin-orbit matrix elements between electronic states of LiRb converging to the third Li(2<sup>2</sup>P) + Rb(5<sup>2</sup>S) dissociation limit; (b) the asymptotic behavior of the present  $\xi_{ij}^{SO}$  values with respect to the  $1/R^6$  coordinate.

the calculations. The self-consistent signs of the *ab initio* SO functions can be obtained using the multiplicative factors from Table II. To simplify the comparison of the present *ab initio* SO functions with their previous theoretical and empirical counterparts, we defined that all SO matrix elements between states converging to the same dissociation limit are positive at large values of  $R$ . This assumption is, however, incorrect for the  $^1\Sigma_0^+ - ^3\Pi_0^+$  and  $^1\Pi_1 - ^3\Pi_1$  matrix elements, since they should both be negative at  $R \rightarrow +\infty$ . Furthermore, according to Table II, the originally calculated SO  $^1\Sigma_0^+ - ^3\Pi_0^+$  and  $^3\Sigma_0^+ - ^3\Pi_0^-$  matrix elements should be multiplied by a factor of  $\sqrt{2}$  to provide the correct fine splitting of the molecular singlet-triplet  $^1\Sigma^+ - ^3\Pi$  and  $^1\Pi - ^3\Pi - ^3\Sigma^+$  complexes near their common dissociation thresholds.

### III. THE ASYMPTOTIC BEHAVIOR OF THE SPIN-ORBIT MATRIX ELEMENTS AS $R \rightarrow +\infty$

The spin-orbit coupling matrix element,  $\xi_{ij}^{SO}$ , between the molecular states  $\psi_i$  and  $\psi_f$  is given by

$$\xi_{ij}^{SO} = \langle \psi_i | H_{SO} | \psi_f \rangle, \quad (1)$$

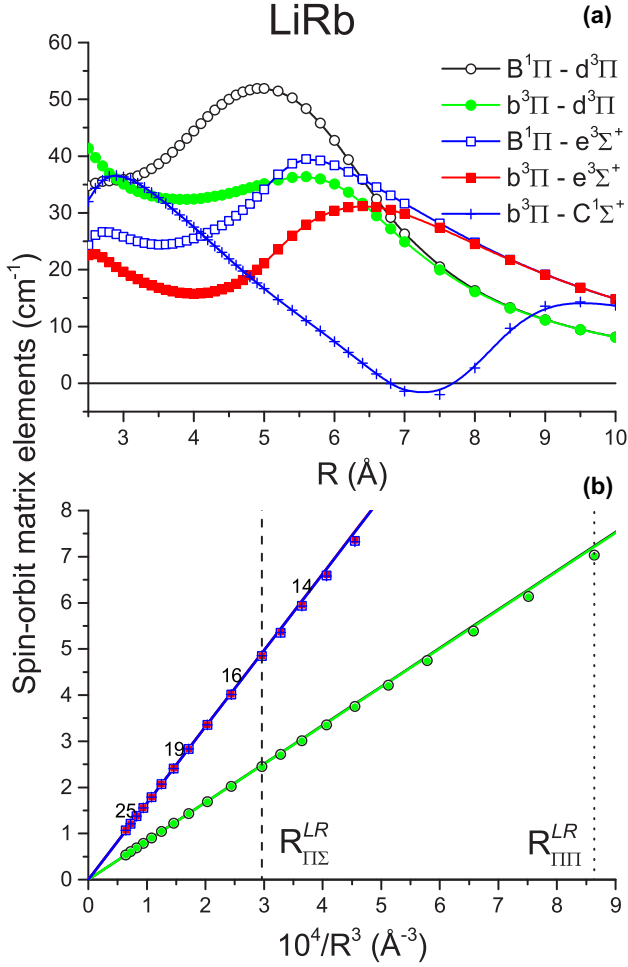


FIG. 3. (a) The present *ab initio* spin-orbit matrix elements between electronic states of LiRb converging to different (the second and third) dissociation limits; (b) the asymptotic behavior of the present  $\xi_{if}^{SO}$  values with respect to the  $1/R^3$  coordinate.

where  $H_{SO}$  is the spin-orbit Hamiltonian that can be split into the atomic  $H_{SO}^{at}$  and interaction  $H_{SO}^{int}$  components:

$$H_{SO} = H_{SO}^{at} + H_{SO}^{int} = H_{SO}^{at}(A) + H_{SO}^{at}(B) + H_{SO}^{int}. \quad (2)$$

In this section,  $H_{SO}$  is assumed to be the microscopic Breit-Pauli spin-orbit Hamiltonian [69] given explicitly in the Appendix, while more approximate forms of the  $H_{SO}$  will be discussed further in the text. In the first step, the interaction component,  $H_{SO}^{int}$ , is neglected leaving only terms resulting from the atomic component,  $H_{SO}^{at}$ .

The expansion of the molecular wave functions  $\psi_i$  and  $\psi_f$  in the perturbation series up to the second order in the intermolecular interaction,  $\hat{V}$ , is given by

$$\psi_{i/f} \approx \psi_{i/f}^{(0)} + \psi_{i/f}^{(1)} + \psi_{i/f}^{(2)}, \quad (3)$$

where the zero-order molecular wave functions are products of the atomic wave functions:  $\psi_i^{(0)} = |i_A\rangle|i_B\rangle$  and  $\psi_f^{(0)} = |f_A\rangle|f_B\rangle$ . The indices A and B denote the isolated atoms, and  $i$  and  $f$  stand for the quantum states of the bra and ket molecular wave functions, respectively.

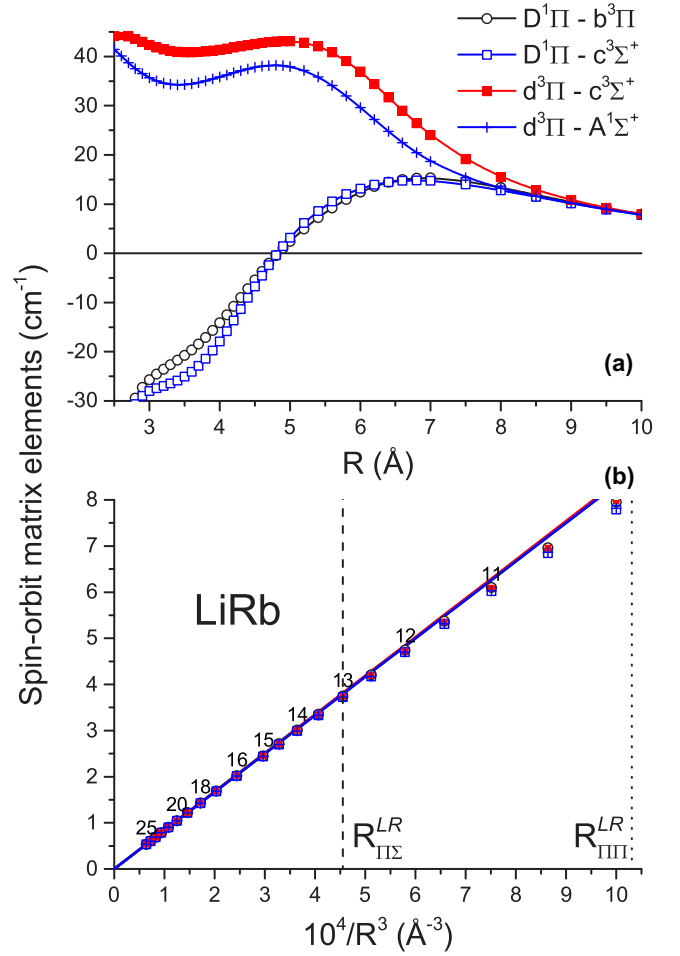


FIG. 4. (a) The present *ab initio* spin-orbit matrix elements between electronic states of LiRb converging to different (the third and second) dissociation limits; (b) the asymptotic behavior of the present  $\xi_{if}^{SO}$  values with respect to the  $1/R^3$  coordinate.

If the interacting species are neutral atoms, then the first-order molecular wave function in its lowest order is due to the dipole-dipole interaction component,  $\hat{V}_{d-d}$ , of the interaction operator,  $\hat{V}$ , which asymptotically decays as  $1/R^3$  with the interatomic distance,  $R$ :

$$\psi_{i/f}^{(1)} = \hat{R}_0 \hat{V}_{d-d} \psi_{i/f}^{(0)}. \quad (4)$$

A similar expression for the second-order molecular wave function is given by

$$\begin{aligned} \psi_{i/f}^{(2)} = & \hat{R}_0 \hat{V}_{d-d} \hat{R}_0 \hat{V}_{d-d} \psi_{i/f}^{(0)} \\ & - \langle \psi_{i/f}^{(0)} | \hat{V}_{d-d} | \psi_{i/f}^{(0)} \rangle \hat{R}_0^2 \hat{V}_{d-d} \psi_{i/f}^{(0)}. \end{aligned} \quad (5)$$

In the above equations, the reduced resolvent operator,  $\hat{R}_0$ , of the dimer AB is defined as

$$\hat{R}_0 = \sum_{n_A \neq i_A} \sum_{n_B \neq i_B} \frac{|n_A\rangle \langle n_B| \langle n_B| \langle n_A|}{\Delta E_{i_A n_A} + \Delta E_{i_B n_B}}, \quad (6)$$

$$\Delta E_{i_A n_A} = E_{i_A} - E_{n_A}, \quad \Delta E_{i_B n_B} = E_{i_B} - E_{n_B}, \quad (7)$$

and the dipole-dipole operator,  $\hat{V}_{d-d}$ , is defined as

$$\hat{V}_{d-d} = -\frac{2d_0^1(A)d_0^1(B) + d_1^1(A)d_{-1}^1(B) + d_{-1}^1(A)d_1^1(B)}{R^3}, \quad (8)$$

where  $d_m^1(X)$  ( $X \equiv A$  or  $B$ ) is the  $m$ th spherical component of the dipole operator for the atom  $X$ , and the molecular fixed  $z$  axis is assumed to parallel the interatomic axis. The indices  $n_A$  and  $n_B$  (or  $n'_A$  and  $n'_B$  used later on) in Eq. (6) are composite labels, i.e., they involve all possible quantum numbers and their projections ( $n, S, M_S, L, M_L$  for the atom  $X$  in its  $n^{2S+1}L$  state). It should also be noted that the expectation value of the dipole-dipole operator Eq. (8) is zero, so in Eq. (5) for the second-order correction  $\psi_{if}^{(2)}$ , only the first term survives.

### A. Initial and final states corresponding to the same dissociation limit

First, the long-range behavior of the SO matrix elements between heteronuclear dimer states converging to the same dissociation limit, i.e.,  $i_A = f_A$  and  $i_B = f_B$ , is considered. To realize that, all terms of the expansion Eq. (3) are inserted into Eq. (1), and only the nonvanishing contributions are retained. The first nonvanishing component is the purely atomic one:

$$\begin{aligned} \langle \psi_i^{(0)} | H_{SO}^{\text{at}} | \psi_f^{(0)} \rangle &= \langle i_A | \langle i_B | (H_{SO}^{\text{at}}(A) + H_{SO}^{\text{at}}(B)) | f_A \rangle | f_B \rangle \\ &= \langle i_A | H_{SO}^{\text{at}} | f_A \rangle + \langle i_B | H_{SO}^{\text{at}} | f_B \rangle = \xi_{\text{at}}. \end{aligned} \quad (9)$$

Since, in the present case, the dissociation limit is equal to  $A(n_A^2P) + B(n_B^2S)$ , only atom  $A$  in the  $n_A^2P$  state (see Table I) yields a zero-order contribution into the molecular SO splitting.

The second leading term comes from matrix elements involving the  $\psi_i^{(0)}$  and  $\psi_f^{(1)}$ , or  $\psi_i^{(1)}$  and  $\psi_f^{(0)}$  wave functions, but it vanishes due to symmetry constraints, namely because the spin-orbit operator connects states of the same parity while the dipole operator acts on states of opposite parity.

The next nonvanishing term arises from the second order of perturbation theory (where the  $\hat{V}_{d-d}$  operator is considered as a perturbation) and it decays asymptotically as  $\beta_{if}^{[6]}/R^6$ :

$$\langle \psi_i^{(1)} | H_{SO}^{\text{at}} | \psi_f^{(1)} \rangle + \langle \psi_i^{(0)} | H_{SO}^{\text{at}} | \psi_f^{(2)} \rangle + \langle \psi_i^{(2)} | H_{SO}^{\text{at}} | \psi_f^{(0)} \rangle = \frac{\beta_{if}^{[6]}}{R^6}, \quad (10)$$

where the long-range coefficient  $\beta_{if}^{[6]}$  consists of three summands:  $\beta_{if}^{[6]}(\text{I})$ ,  $\beta_{if}^{[6]}(\text{II})$ , and  $\beta_{if}^{[6]}(\text{III})$ .

The  $\beta_{if}^{[6]}(\text{I})$  term corresponds to the first matrix element in Eq. (10):

$$\langle \psi_i^{(1)} | H_{SO}^{\text{at}} | \psi_f^{(1)} \rangle = \langle \psi_i^{(0)} | \hat{V}_{d-d} \hat{R}_0 H_{SO}^{\text{at}} \hat{R}_0 \hat{V}_{d-d} | \psi_f^{(0)} \rangle = \frac{\beta_{if}^{[6]}(\text{I})}{R^6}, \quad (11)$$

and it can be expressed as the sum-over-states:

$$\beta_{if}^{[6]}(\text{I}) = \sum_{m,m'=-1}^1 \sum_{n_A \neq i_A} \sum_{n_B \neq i_B} \sum_{n'_A \neq f_A} C_{mm'} \frac{\langle i_A | d_m^1 | n_A \rangle \langle n_A | H_{SO}^{\text{at}}(A) | n'_A \rangle \langle n'_A | d_{m'}^1 | f_A \rangle \langle i_B | d_{-m}^1 | n_B \rangle \langle n_B | d_{-m'}^1 | f_B \rangle}{(\Delta E_{i_A n_A} + \Delta E_{i_B n_B})(\Delta E_{f_A n'_A} + \Delta E_{f_B n_B})} + (A \leftrightarrow B), \quad (12)$$

where  $C_{00} = 4$ ,  $C_{01} = C_{0-1} = C_{10} = C_{-10} = 2$ , and  $C_{11} = C_{1-1} = C_{-11} = C_{-1-1} = 1$ , and the expression  $(A \leftrightarrow B)$ , hereafter, means an extra term with all indices related to the atom  $A$  replaced by the equivalent indices of the atom  $B$  and vice versa.

The second term summand results from the atomic SO coupling between the  $\psi_i^{(0)}$  and  $\psi_f^{(2)}$  states:

$$\langle \psi_i^{(0)} | H_{SO}^{\text{at}} | \psi_f^{(2)} \rangle = \langle \psi_i^{(0)} | H_{SO}^{\text{at}} \hat{R}_0 \hat{V}_{d-d} \hat{R}_0 \hat{V}_{d-d} | \psi_f^{(0)} \rangle = \frac{\beta_{if}^{[6]}(\text{II})}{R^6}, \quad (13)$$

where the coefficient  $\beta_{if}^{[6]}(\text{II})$  is given by

$$\beta_{if}^{[6]}(\text{II}) = \sum_{m,m'=-1}^1 \sum_{n_A \neq f_A} \sum_{n_B \neq f_B} \sum_{n'_A \neq f_A} C_{mm'} \frac{\langle i_A | H_{SO}^{\text{at}}(A) | n'_A \rangle \langle n'_A | d_m^1 | n_A \rangle \langle n_A | d_{m'}^1 | f_A \rangle \langle i_B | d_{-m}^1 | n_B \rangle \langle n_B | d_{-m'}^1 | f_B \rangle}{\Delta E_{f_A n'_A} (\Delta E_{f_A n_A} + \Delta E_{f_B n_B})} + (A \leftrightarrow B). \quad (14)$$

The last term results from the SO coupling between the  $\psi_i^{(2)}$  and  $\psi_i^{(0)}$  states:

$$\langle \psi_i^{(2)} | H_{SO}^{\text{at}} | \psi_f^{(0)} \rangle = \langle \psi_i^{(0)} | \hat{V}_{d-d} \hat{R}_0 \hat{V}_{d-d} \hat{R}_0 H_{SO}^{\text{at}} | \psi_f^{(0)} \rangle = \frac{\beta_{if}^{[6]}(\text{III})}{R^6}, \quad (15)$$

where the expression for  $\beta_{if}^{[6]}(\text{III})$  is the same as Eq. (14) except for the interchange of the  $i$  and  $f$  states.

### B. Initial and final states corresponding to different dissociation limits

Now, it shall be assumed that the SO coupled  $\psi_i$  and  $\psi_f$  states converge to different dissociation limits. This means that  $i_A \neq f_A$ ,  $i_B \neq f_B$  and there is no pure atomic contribution to the SO matrix elements. The first nonvanishing term in the long-range

expansion of  $\xi_{if}^{SO}$  arises from the first-order wave functions  $\psi_i^{(1)}$  or  $\psi_f^{(1)}$ , and it drops off asymptotically as a function of  $1/R^3$ :

$$\langle \psi_i^{(0)} | H_{SO}^{at} | \psi_f^{(1)} \rangle + \langle \psi_i^{(1)} | H_{SO}^{at} | \psi_f^{(0)} \rangle = \langle \psi_i^{(0)} | H_{SO}^{at} \hat{R}_0 \hat{V}_{d-d} | \psi_f^{(0)} \rangle + \langle \psi_i^{(0)} | \hat{V}_{d-d} \hat{R}_0 H_{SO}^{at} | \psi_f^{(0)} \rangle = \frac{\beta_{if}^{[3]}(\text{I}) + \beta_{if}^{[3]}(\text{II})}{R^3} = \frac{\beta_{if}^{[3]}}{R^3}, \quad (16)$$

where the coefficient  $\beta_{if}^{[3]}(\text{I})$  can be expanded in the sum-over-states:

$$\beta_{if}^{[3]}(\text{I}) = \sum_{m=-1}^1 \sum_{n_A \neq f_A} D_m \frac{\langle i_A | H_{SO}^{at}(\text{A}) | n_A \rangle \langle n_A | d_m^1 | f_A \rangle \langle i_B | d_{-m}^1 | f_B \rangle}{\Delta E_{f_A n_A} + \Delta E_{f_B i_B}} + (\text{A} \leftrightarrow \text{B}), \quad (17)$$

where the coefficients,  $D_m$ , are defined as  $D_0 = -2$  and  $D_1 = D_{-1} = -1$ . An analogous expression for  $\beta_{if}^{[3]}(\text{II})$  can be obtained from Eq. (17) by interchanging the indices corresponding to the states  $\psi_i$  and  $\psi_f$ .

### C. Contributions of the intermolecular spin-orbit interaction

So far, the derived long-range expressions have not depended on the particular form of the spin-orbit Hamiltonian used, i.e., they work when  $H_{SO}^{at}$  is taken in the Breit-Pauli form [69] or as an effective core potential (although the actual numerical values may, obviously, differ). The interaction component,  $H_{SO}^{int}$ , of the Hamiltonian Eq. (2) incorporates the SO interaction between electrons from different atoms. In this subsection, the leading  $R^{-k}$  contribution arising from the multipole expansion of the  $H_{SO}^{int}$  operator are derived, since this has not been reported in literature yet. Fontana and Meath [70] considered the one-center expansion, while Meath [71] derived a few leading terms in the two-center expansion. See Hirschfelder and Meath [72] for the review of the multipole expansion of various relativistic operators.

The multipole expansion of the operator  $H_{SO}^{int}$  is given by the following expression:

$$H_{SO}^{int} = \sum_{l_A=0}^{\infty} \sum_{l_B=0}^{\infty} \frac{i\sqrt{6}}{2 R^{l_A+l_B+2}} [1 + \hat{P}(\text{A}, \text{B}) (-1)^{l_A+l_B+1}] \left\{ \sum_{\lambda} \tau_{\lambda}^{l_A, l_B} \left[ \mathbf{Q}^{l_B}(\text{B}) \otimes \sum_{j \in \text{A}} [\mathbf{R}^{l_A}(\vec{r}_j) \otimes [\mathbf{p}^1(\vec{r}_j) \otimes \mathbf{s}^1(j)]^1]^{\lambda} \right]_0^{l_A+l_B+1} \right. \\ \left. + 2 \sum_{\lambda, \lambda'} \gamma_{\lambda, \lambda'}^{l_A, l_B} \left[ \sum_{k \in \text{B}} [\mathbf{R}^{l_B}(\vec{r}_k) \otimes \mathbf{p}^1(\vec{r}_k)]^{\lambda} \otimes \sum_{j \in \text{A}} [\mathbf{R}^{l_A}(\vec{r}_j) \otimes \mathbf{s}^1(j)]^{\lambda'} \right]_0^{l_A+l_B+1} \right\}, \quad (18)$$

where  $\hat{P}(\text{A}, \text{B})$  is the operator interchanging the indices of the monomers A and B. Note that Eq. (18) was derived in the spirit of the derivation of Wormer [31] for the multipole expansion of the intermolecular interaction operator,  $\hat{V}$ , with the full recoupling of the spherical tensors in such a way that operators acting on the coordinates of the monomers A and B are explicitly separated. A sketch of the derivation of Eq. (18) together with an explanation of all symbols used is reported in the Appendix.

Assuming an effective single electron on each of the uncharged monomers, the  $R^{-3}$  term arising from Eq. (18) reads

$$H_{SO}^{int} = \frac{i\sqrt{6}}{2 R^3} \sum_{m=-1}^1 \sum_{m_1, m_2=-1}^1 \langle 1m_1 1m_2 | 1m \rangle \left\{ -\sqrt{2} \langle 1-m 1m | 20 \rangle d_{-m}^1(\text{A}) p_{m_1}^1(\vec{r}_B) s_{m_2}^1(\text{B}) \right. \\ \left. + [p_{-m}^1(\vec{r}_B) R_{m_1}^1(\vec{r}_A) s_{m_2}^1(\text{A}) + R_{m_1}^1(\vec{r}_A) p_{m_2}^1(\vec{r}_B) s_{-m}^1(\text{B})] \left( \sqrt{\frac{2}{3}} \langle 1-m 1m | 20 \rangle + \frac{1}{\sqrt{2}} \langle 1-m 2m | 20 \rangle \right) \right\} \\ + (\text{A} \leftrightarrow \text{B}) + \mathcal{O}(R^{-4}). \quad (19)$$

Combining the above relation Eq. (19) to Eq. (16) leads to the following  $\delta\beta_{if}^{[3]}$  correction to the  $\beta_{if}^{[3]}$  values:

$$\delta\beta_{if}^{[3]} = -\frac{\sqrt{6}}{2} \sum_{m=-1}^1 \sum_{m_1, m_2=-1}^1 \langle 1m_1 1m_2 | 1m \rangle \left[ (\sqrt{2} \Delta E_{i_B f_B} + \sqrt{\frac{2}{3}} \Delta E_{i_A f_A}) \langle 1-m 1m | 20 \rangle + \frac{1}{\sqrt{2}} \Delta E_{i_A f_A} \langle 1-m 2m | 20 \rangle \right] \\ \times \langle i_A | d_{-m}^1 | f_A \rangle \langle i_B | d_{m_1}^1 s_{m_2}^1(\text{B}) | f_B \rangle + (\text{A} \leftrightarrow \text{B}), \quad (20)$$

where the identities  $\langle i_X | s_m^1 | f_X \rangle = 0$  and  $\langle i_X | p_m^1 | f_X \rangle = i \Delta E_{i_X f_X} \langle i_X | d_m^1 | f_X \rangle$  ( $X \equiv \text{A}$  or  $\text{B}$ ) are used.

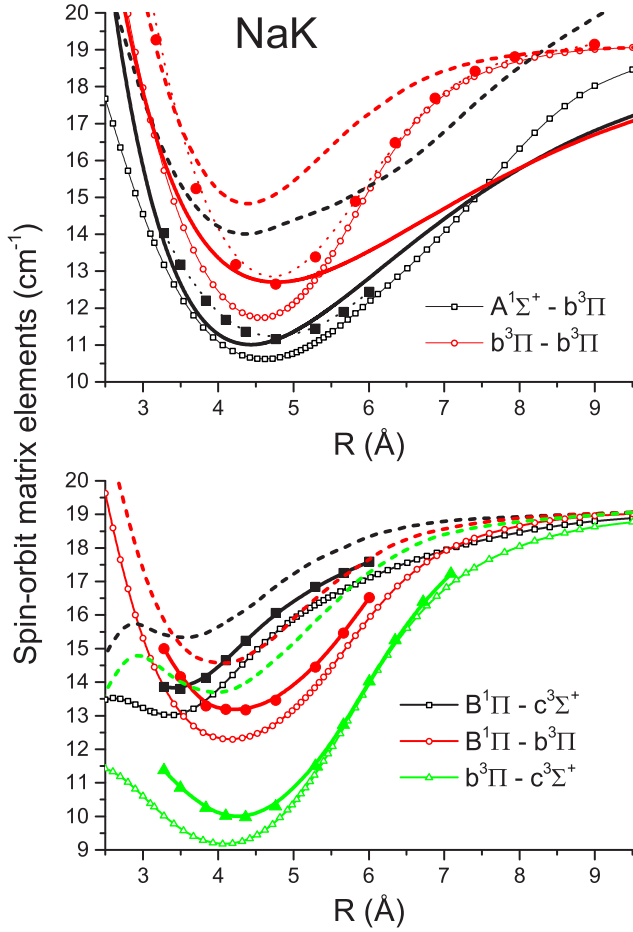


FIG. 5. Comparison of the theoretical and experimental spin-orbit matrix elements available for the NaK states converging to the second  $\text{Na}(3^2\text{S}) + \text{K}(4^2\text{P})$  dissociation limit. The solid lines indicate the empirical SO functions obtained during the coupled-channel deperturbation analysis of the  $A^1\Sigma^+ - b^3\Pi$  complex [21]. The open symbols are results of the present work. The solid symbols corresponds the *ab initio* estimates derived in a limited range of  $R$  during an ECP-MPPT calculation [19]. The dashed lines denote the *ab initio* results of the full electron BP-MRCI calculations [20]. The original SO functions borrowed from Ref. [20] are uniformly scaled here to reach the correct (experimental) atomic asymptote,  $\text{K}(4^2\text{P})$ .

#### IV. DISCUSSION

The analytical results obtained within the framework of the long-range perturbation theory lead to the following propensity rules for the asymptotic behavior of the SO matrix elements,  $\xi_{if}^{\text{SO}}$ :

(1) for the molecular states of AB converging to the same  $A(n_A^2\text{P}) + B(n_B^2\text{S})$  dissociation limit

$$\xi_{if}^{\text{SO}}(R \rightarrow +\infty) \rightarrow \xi_{n_A^2\text{P}}^{\text{SO}} + \frac{\beta_{if}^{[6]}}{R^6}, \quad (21)$$

where  $\xi_{n_A^2\text{P}}^{\text{SO}}$  is the SO splitting parameter of atom A in the  $n^2\text{P}$  state;

(2) for the molecular states of AB corresponding to the  $A(n_A^2\text{P}) + B(n_B^2\text{S})$  and  $A(n_A^2\text{S}) + B(n_B^2\text{P})$  dissociation

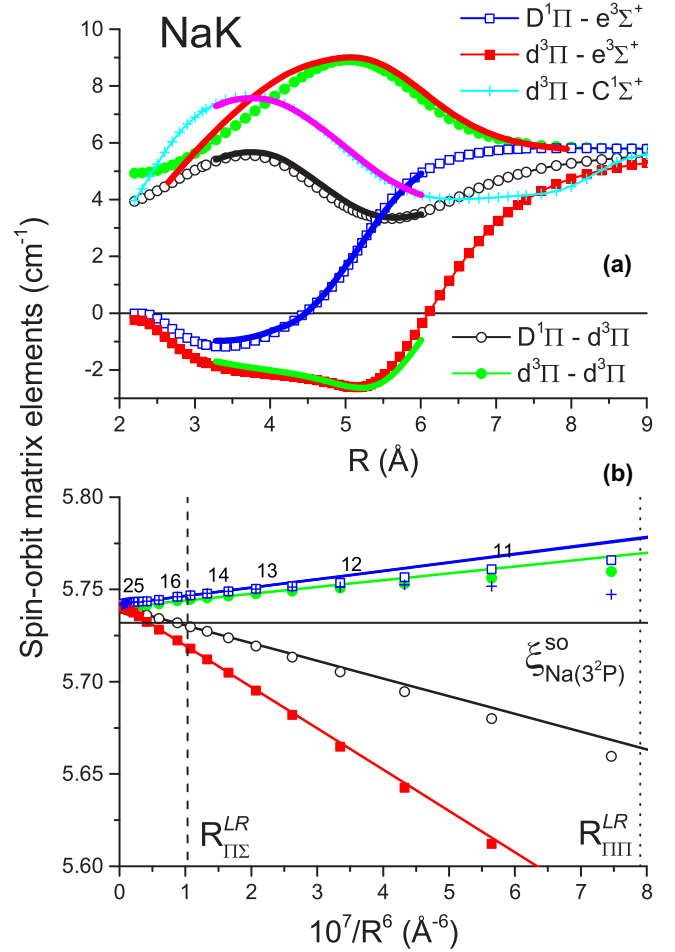


FIG. 6. (a) The present *ab initio* spin-orbit matrix elements between the NaK states converging to the third  $\text{Na}(3^2\text{P}) + \text{K}(4^2\text{S})$  dissociation limit. The solid lines indicate the SO functions obtained within the framework of an ECP-MPPT calculation [18]; (b) the asymptotic behavior of the present  $\xi_{if}^{\text{SO}}$  values with respect to the  $1/R^6$  coordinate.

tion thresholds the SO function is reduced to

$$\xi_{if}^{\text{SO}}(R \rightarrow +\infty) \rightarrow \frac{\beta_{if}^{[3]}}{R^3}; \quad (22)$$

The spin-orbit coupling matrix elements  $\xi_{if}^{\text{SO}}(R)$  between electronic states converging to the second  $A(n_A^2\text{P}) + B(n_B^2\text{S})$  ( $A^1\Sigma^+$ ,  $B^1\Pi$ ,  $b^3\Pi$ ,  $c^3\Sigma^+$ ) and third  $A(n_A^2\text{S}) + B(n_B^2\text{P})$  ( $C^1\Sigma^+$ ,  $D^1\Pi$ ,  $d^3\Pi$ ,  $e^3\Sigma^+$ ) state manifolds of the alkali mixed dimers  $\text{AB}$  ( $A, B = \text{Li, Na, K, Rb}$ ) were evaluated over a wide range of internuclear distances,  $R$ , namely:  $R \in [2.2, 35] \text{ \AA}$  for  $\text{KRb}$  and  $R \in [2, 25] \text{ \AA}$  for all others. The resulting *ab initio* SO functions for the  $\text{LiNa}$ ,  $\text{LiK}$ ,  $\text{LiRb}$ ,  $\text{NaK}$ ,  $\text{NaRb}$ , and  $\text{KRb}$  molecules are presented graphically and tabulated in point-wise format in Supplemental Material (SM) [73]. The long-range portion of the same *ab initio*  $\xi_{if}^{\text{SO}}(R)$  functions are represented in the lower half of the same figures with respect to the reciprocal  $1/R^3$  or  $1/R^6$  coordinates. The vertical (dashed and dotted) lines mark the modified LeRoy radius [40] ( $R_{\Sigma-\Pi}^{\text{LR}}$  and  $R_{\Pi-\Pi}^{\text{LR}}$ ) estimated for the  $\Sigma-\Pi$  and  $\Pi-\Pi$  matrix elements, respectively (see Ref. [39] for details).

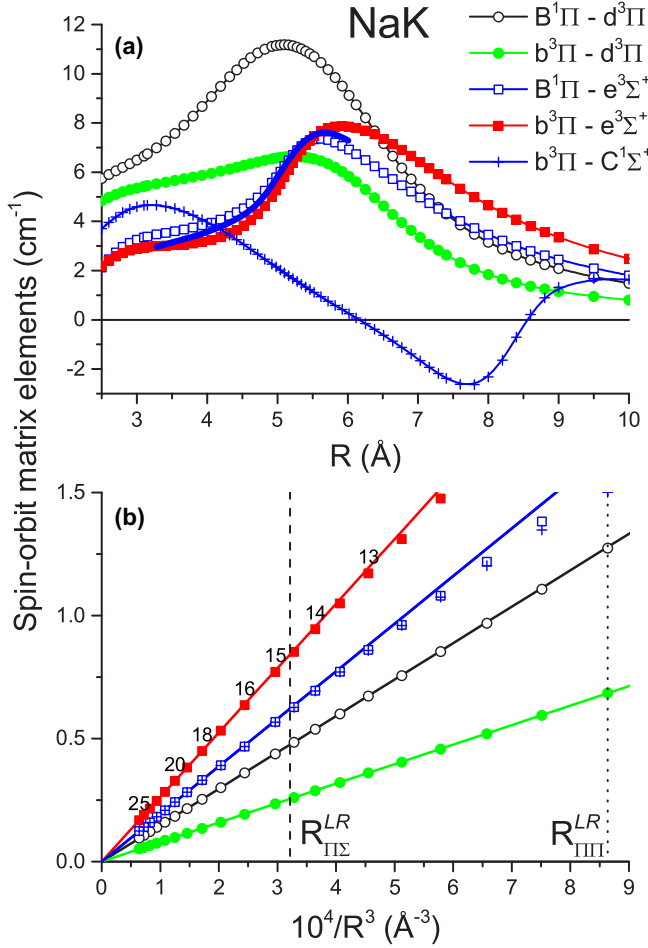


FIG. 7. (a) The present *ab initio* spin-orbit matrix elements between electronic states of NaK converging to different (the second and third) dissociation limits. The solid line indicates the SO functions obtained within the framework of an ECP-MPPT calculation [18,19]; (b) the asymptotic behavior of the present  $\xi_{if}^{SO}$  values with respect to the  $1/R^3$  coordinate.

The horizontal lines denote the experimental SO parameters of the corresponding alkali atoms [67],  $\xi_{nA^2P}^{\text{exp}}$ , given in Table I. The selected  $\xi_{if}^{SO}(R)$  functions of the LiRb, NaK, NaRb, and KRb molecules are depicted on Figs. 1–10 for illustrative purposes.

It is easily seen that the vast majority of the derived *ab initio* SO matrix elements demonstrate a pronounced  $R$ -dependence over the entire range of interatomic distances. Indeed, at small and intermediate distances,  $R$ , the absolute magnitude of the SO molecular functions could deviate significantly from their asymptotic counterparts corresponding to  $R \rightarrow +\infty$ . The extremely sharp changes of the SO matrix elements involving the lowest  $^1\Pi$  states of the KRb molecule [see Fig. 10(a)] are due to the avoided crossing effect [74] of the adiabatic  $B^1\Pi$  and  $D^1\Pi$  states around  $R \approx 5.5$  Å. It should be noted that, for the KRb molecule, the SO long-range expansion becomes valid at abnormally large interatomic distances significantly exceeding the LeRoy radius estimates [see, for instance, Fig. 10(b)]. The latter was observed for the ETDM functions, as well [39]. The effect could be attributed

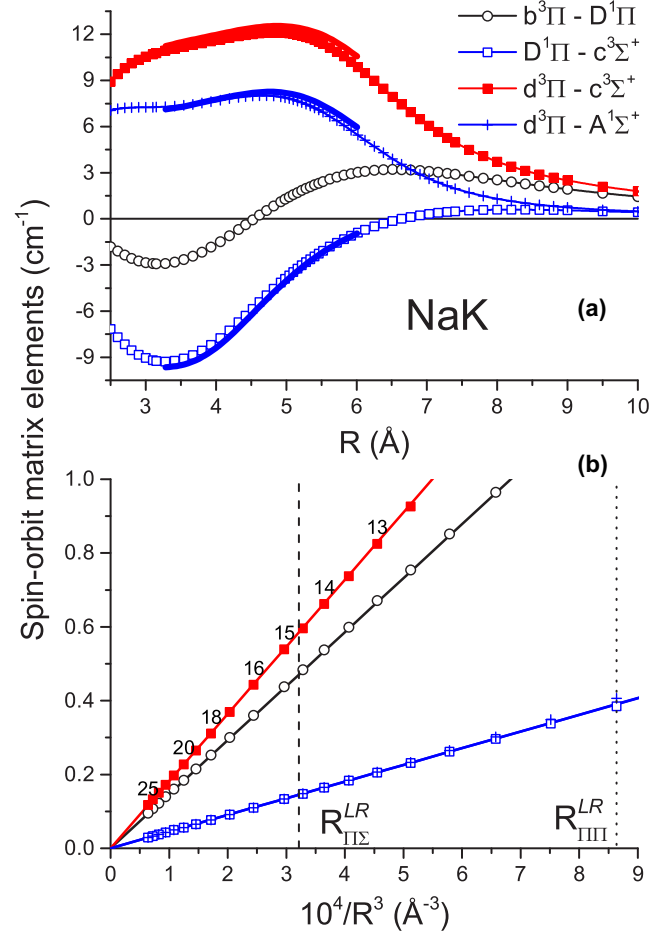


FIG. 8. (a) The present *ab initio* spin-orbit matrix elements between electronic states of NaK converging to different (the third and second) dissociation limits. The solid lines indicate the theoretical SO functions obtained within the framework of an ECP-MPPT calculation [18,19]; (b) the asymptotic behavior of the present  $\xi_{if}^{SO}$  values with respect to the  $1/R^3$  coordinate.

to the prolonging electronic correlation caused by the proximity of the second and third dissociation thresholds to each other (see Table I).

At intermediate distances both present *ab initio* diagonal  $b^3\Pi-b^3\Pi$  and off-diagonal  $A^1\Sigma^+-b^3\Pi$  SO matrix elements calculated for the NaK, NaRb, and KRb molecules agree very well with their empirical counterparts obtained within the framework of the highly accurate coupled-channel deperturbation analysis of the rovibronic term values belonging to the singlet-triplet  $A^1\Sigma^+ \sim b^3\Pi$  complex [21,23,24]. The present SO splitting function for the  $d^3\Pi$  state and SO coupling matrix element of the states  $D^1\Pi-d^3\Pi$  for the NaK molecule are also in good agreement with empirical estimates obtained using the effective Hamiltonian deperturbation treatment [18] of the experimental rovibronic term values of the NaK  $D^1\Pi \sim d^3\Pi$  complex [25]. The present SO functions for the NaK and NaRb molecules are remarkably close to previous estimates [18,19,22,23] obtained within the framework of the multipartition perturbation theory (MPPT) calculation. At the same time, the present SO matrix elements systematically underestimate the previous NaK results [20]



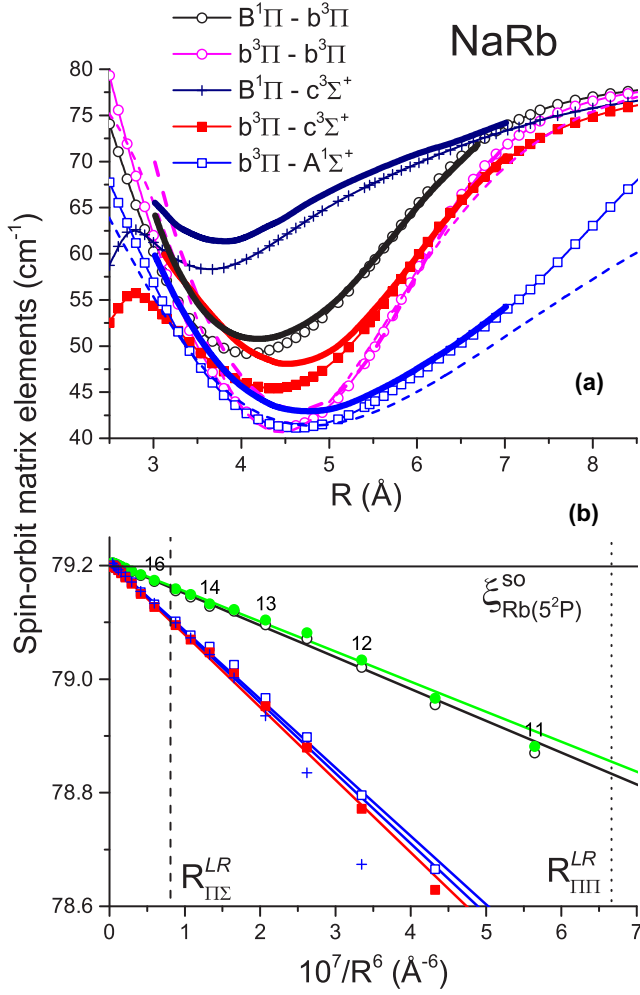


FIG. 9. (a) Comparison of the theoretical and experimental spin-orbit matrix elements for the NaRb states converging to the second Na(3<sup>2</sup>S) + Rb(5<sup>2</sup>P) dissociation limit. The dash lines indicate the empirical SO functions obtained during the CC deperturbation analysis of the A<sup>1</sup>Σ<sup>+</sup> - b<sup>3</sup>Π complex [23]. The symbols are results of the present work. The solid lines correspond the *ab initio* ECP-MPPT estimates [22]; (b) the asymptotic behavior of the present  $\xi_{ij}^{\text{SO}}$  values with respect to the 1/R<sup>6</sup> coordinate.

obtained within the full electron multireference configuration interaction (MRCI) calculations based on the microscopic Breit-Pauli (BP) Hamiltonian.

The present *ab initio* SO functions obtained between molecular states converging to the same and to different atomic thresholds could all be approximated quite accurately at large distances using the asymptotic Eqs. (21) and (22), respectively. The relevant long-range expansion coefficients  $\beta_{if}^{[6]}$  and  $\beta_{if}^{[3]}$ , obtained by performing a linear least squares fit of the present SO matrix elements are given in Tables III and IV, respectively. The reliability of the present *ab initio* SO functions is confirmed by the good agreement of the fitting parameters,  $\xi_{n^2p}^{\text{calc}}$ , with the corresponding experimental atomic values,  $\xi_{n^2p}^{\text{exp}}$ , from Table I.

As follows from long-range theory, the derived  $|\beta_{if}^{[n]}|$  values given in Tables III and IV generally demonstrate that they are independent of the S and Σ quantum numbers for

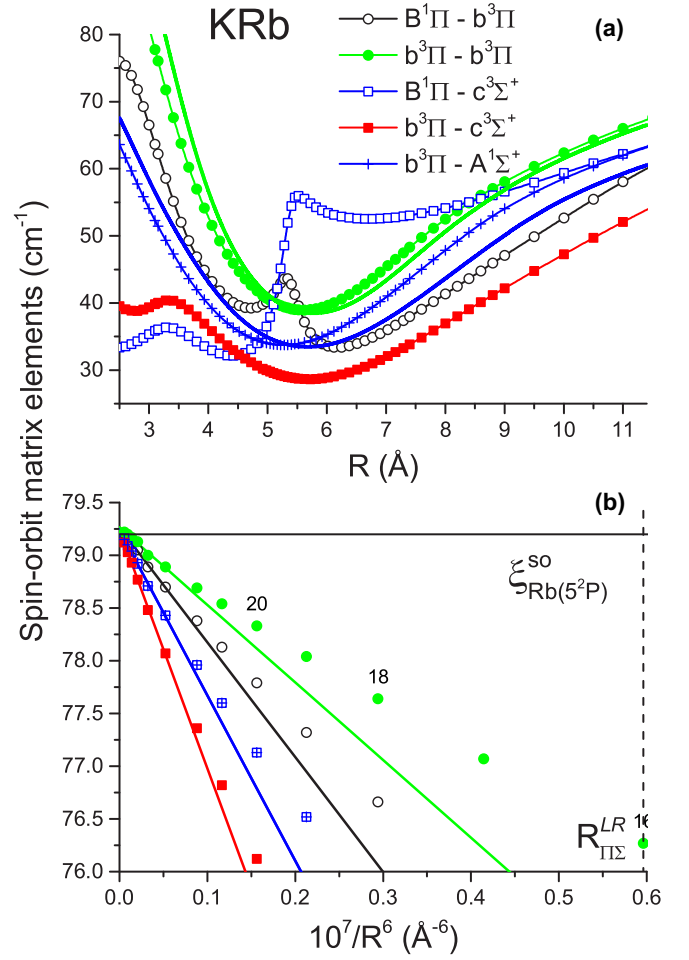


FIG. 10. (a) The present *ab initio* spin-orbit matrix elements between the KRb states converging to the second K(4<sup>2</sup>S) + Rb(5<sup>2</sup>P) dissociation limit. The solid lines indicate the empirical SO functions obtained by means of the CC deperturbation analysis of the A<sup>1</sup>Σ<sup>+</sup> - b<sup>3</sup>Π complex [24]; (b) the asymptotic behavior of the present  $\xi_{ij}^{\text{SO}}$  values with respect to the 1/R<sup>6</sup> coordinate.

most states. This tendency holds true for the Li-containing molecules, but some exceptions arise for the triplet-triplet Π-Σ and Π-Π transitions for the heavier molecules NaK, NaRb, and KRb. Furthermore, the  $\beta_{if}^{[3]}$  coefficients of LiNa, LiK, and LiRb molecules for states corresponding to the excited Li(2<sup>2</sup>P) atom almost coincide for Π-Σ and Π-Π transitions, and their values are approximately two times smaller than the  $\beta_{if}^{[3]}$  values corresponding to the atomic ground state Li(2<sup>2</sup>S) (see Table IV). A reason of the observed peculiarities is not evident for the moment.

Table V contains the contribution to the asymptotic coefficients,  $\beta_{if}^{[3]}$ , arising from the multipole expansion of the intermolecular Breit-Pauli Hamiltonian,  $H_{\text{SO}}^{\text{int}}$ , i.e., terms neglected when effective core potentials are used in the calculations. An inspection of Table V shows that the corrections resulting from the microscopic electron-electron spin-orbit interaction are several orders of magnitude smaller than  $\beta_{if}^{[3]}$  (see Table IV) resulting from  $H_{\text{SO}}^{\text{at}}$ . This is a very encouraging result, since calculations involving  $H_{\text{SO}}^{\text{int}}$  beyond the effective

TABLE III. Long-range expansion coefficients,  $\beta_{if}^{[6]}$  (in  $\text{cm}^{-1} \text{\AA}^6$ ), obtained using Eq. (21) from the present *ab initio* SO matrix elements between the molecular states converging to the second and third dissociation thresholds. The numbers in the square brackets denote powers of ten.

	LiNa	LiK	LiRb	NaK	NaRb	KRb
$B^1\Pi - e^3\Sigma^+$	9.757[4]	-7.408[5]	-2.665[6]	-2.432[5]	-1.206[6]	-1.568[8]
$b^3\Pi - A^1\Sigma^+$	9.757[4]	-7.412[5]	-2.687[6]	-2.400[5]	-1.243[6]	-1.572[8]
$b^3\Pi - e^3\Sigma^+$	-1.024[5]	-7.447[5]	-2.671[6]	-3.264[5]	-1.278[6]	-2.276[8]
$D^1\Pi - e^3\Sigma^+$	-1.406[5]	5.415[5]	1.722[6]	4.495[4]	4.297[5]	1.056[8]
$d^3\Pi - C^1\Sigma^+$	-1.406[5]	5.415[5]	1.723[6]	4.570[4]	4.239[5]	1.056[8]
$d^3\Pi - e^3\Sigma^+$	-1.432[5]	-5.472[5]	-1.800[6]	-2.239[5]	-5.798[5]	-1.791[8]
$B^1\Pi - b^3\Pi$	-5.107[4]	-3.308[5]	-1.178[6]	-1.484[5]	-5.607[5]	-1.009[8]
$b^3\Pi - b^3\Pi$	4.981[4]	-3.315[5]	-1.174[6]	-1.073[5]	-5.290[5]	-7.364[7]
$D^1\Pi - d^3\Pi$	-6.153[4]	-2.683[5]	-8.680[5]	-9.602[4]	2.057[5]	-8.487[7]
$d^3\Pi - d^3\Pi$	-6.256[4]	2.769[5]	8.665[5]	3.691[4]	-2.977[5]	6.123[7]

TABLE IV. Long-range expansion coefficients,  $\beta_{if}^{[3]}$  (in  $\text{cm}^{-1} \text{\AA}^3$ ), obtained using Eq. (22) from the present *ab initio* SO matrix elements between molecular states corresponding to the second  $A(n_A^2P) + B(n_B^2S)$  and third  $A(n_A^2S) + B(n_B^2P)$  dissociation thresholds, respectively. The numbers in the square brackets denote powers of ten.

	LiNa	LiK	LiRb	NaK	NaRb	KRb
$B^1\Pi - e^3\Sigma^+$	5.178[2]	4.529[3]	1.656[4]	1.935[3]	8.305[3]	1.335[5]
$b^3\Pi - C^1\Sigma^+$	5.178[2]	4.530[3]	1.657[4]	1.934[3]	8.274[3]	1.337[5]
$b^3\Pi - e^3\Sigma^+$	5.578[2]	4.553[3]	1.659[4]	2.622[3]	8.956[3]	1.709[5]
$D^1\Pi - e^3\Sigma^+$	1.064[3]	2.255[3]	8.335[3]	4.522[2]	3.824[3]	3.975[4]
$d^3\Pi - A^1\Sigma^+$	1.063[3]	2.255[3]	8.335[3]	4.522[2]	3.824[3]	3.974[4]
$d^3\Pi - e^3\Sigma^+$	1.084[3]	2.302[3]	8.378[3]	1.821[3]	5.135[3]	1.137[5]
$B^1\Pi - d^3\Pi$	5.480[2]	2.292[3]	8.369[3]	1.480[3]	4.758[3]	9.562[4]
$D^1\Pi - b^3\Pi$	5.478[2]	2.269[3]	8.370[3]	1.480[3]	4.809[3]	9.561[4]
$b^3\Pi - d^3\Pi$	5.280[2]	2.269[3]	8.348[3]	7.925[2]	4.150[3]	5.825[4]

TABLE V. The contribution to the long-range coefficient,  $\delta\beta_{if}^{[3]}$  (in  $\text{cm}^{-1} \text{\AA}^3$ ), arising from the multipole expansion of the intermolecular spin-orbit operator,  $H_{SO}^{int}$ , Eq. (20).

	LiNa	LiK	LiRb	NaK	NaRb	KRb
$B^1\Pi - e^3\Sigma^+$	-0.239	-0.245	-0.233	-0.168	-0.153	-0.394
$b^3\Pi - C^1\Sigma^+$	-0.239	-0.245	-0.233	-0.168	-0.153	-0.394
$b^3\Pi - e^3\Sigma^+$	-0.239	-0.245	-0.233	-0.168	-0.153	-0.394
$D^1\Pi - e^3\Sigma^+$	-0.426	-0.448	-0.474	-0.617	-0.649	-0.433
$d^3\Pi - A^1\Sigma^+$	-0.426	-0.448	-0.474	-0.617	-0.649	-0.433
$d^3\Pi - e^3\Sigma^+$	-0.426	-0.448	-0.474	-0.617	-0.649	-0.433
$B^1\Pi - d^3\Pi$	-0.175	-0.183	-0.190	-0.231	-0.240	-0.196
$D^1\Pi - b^3\Pi$	-0.175	-0.183	-0.190	-0.231	-0.240	-0.196
$b^3\Pi - d^3\Pi$	-0.175	-0.183	-0.190	-0.231	-0.240	-0.196

one-electron treatment would require nonstandard integrals involving products of a number of operators acting simultaneously on the spatial and spin coordinates of electrons, which is not realized in any standard program for electronic structure calculations.

### V. CONCLUDING REMARKS

The spin-orbit matrix elements between the lowest excited electronic states of the heteronuclear alkali metal dimers AB (A, B = Li, Na, K, Rb) were systematically evaluated in a wide range of interatomic distances. Wherever possible, the reliability of the derived *ab initio* SO functions was confirmed through comparison with previous theoretical and empirical results.

The numerical studies of the asymptotic  $R \rightarrow +\infty$  behavior of the calculated  $\xi_{if}^{SO}(R)$  functions were generally supported by the analytical results obtained within the framework of the long-range perturbation theory. The propensity rules for the behavior of the SO long-range coefficients,  $\beta_{if}^{[k]}$ , as an implicit function of the  $S$ ,  $\Sigma$ , and  $\Lambda$  quantum numbers of the  $i$  and  $f$  coupled states were established. Additional  $R^{-3}$  contributions resulting from the intermolecular SO interaction in the Breit-Pauli Hamiltonian were estimated using an effective one-electron model and were shown to be negligible.

It is believed that the overall accuracy of the present *ab initio*  $\xi_{if}^{SO}(R)$  functions should be sufficient to accomplish a comprehensive coupled-channel deperturbation treatment of

the singlet-triplet states manifold of the lightest alkali AB dimers up to the first three dissociation thresholds.

### ACKNOWLEDGMENTS

The study was supported by Russian Foundation for Basic Research (RFBR) Grants No. 16-03-00529 and No. 18-33-00753. R.M. thanks the Polish National Science Center for support through Project No. 2017/25/B/ST4/02698.

### APPENDIX: DERIVATION OF THE MULTIPOLE EXPANSION OF THE INTERACTION SO HAMILTONIAN

The Breit-Pauli spin-orbit Hamiltonian is given by [69]

$$H_{SO} = \frac{1}{2} \sum_{\alpha} \sum_j \frac{Z_{\alpha}}{r_{j\alpha}^3} (\mathbf{r}_{j\alpha} \times \mathbf{p}_j) \cdot \mathbf{s}_j - \frac{1}{2} \sum_{j \neq k} \frac{1}{r_{jk}^3} [(\mathbf{r}_{jk} \times \mathbf{p}_j) \cdot \mathbf{s}_j - 2(\mathbf{r}_{jk} \times \mathbf{p}_k) \cdot \mathbf{s}_j], \quad (A1)$$

where indices  $\alpha$  and  $j$  iterate over all nuclei and electrons,  $Z_{\alpha}$  is the charge of the nucleus  $\alpha$ ,  $\mathbf{r}_{uv}$  is a vector connecting particles  $u$  and  $v$ , and  $\mathbf{p}$  and  $\mathbf{s}$  are the momentum and spin operators. The Hamiltonian,  $H_{SO}$ , can be divided into atomic,  $H_{SO}^{at}$ , and interaction,  $H_{SO}^{int}$ , components:

$$H_{SO} = H_{SO}^A + H_{SO}^B + H_{SO}^{int}, \quad (A2)$$

where the interaction part is defined as

$$H_{SO}^{int} = \frac{1}{2} \sum_{\alpha \in A} \sum_{j \in B} \frac{Z_{\alpha}}{r_{j\alpha}^3} (\mathbf{r}_{j\alpha} \times \mathbf{p}_j) \cdot \mathbf{s}_j - \frac{1}{2} \sum_{j \in A} \sum_{k \in B} \frac{1}{r_{jk}^3} [(\mathbf{r}_{jk} \times \mathbf{p}_j) \cdot \mathbf{s}_j - 2(\mathbf{r}_{jk} \times \mathbf{p}_k) \cdot \mathbf{s}_j] + (A \leftrightarrow B). \quad (A3)$$

An arbitrary vector,  $\mathbf{X}$ , can be expressed as an irreducible tensor operator:

$$T_0^1(\mathbf{X}) = X_z \quad T_{\pm 1}^1(\mathbf{X}) = \mp \frac{1}{\sqrt{2}} (X_x \pm i X_y), \quad (A4)$$

and the irreducible tensor product is defined by the expression

$$[\mathbf{X}^l \otimes \mathbf{Y}^{l'}]_{\lambda'}^{\lambda} \equiv \sum_{m=-l}^l \sum_{m'=-l'}^{l'} \langle l, m; l', m' | \lambda, \lambda' \rangle X_m^l Y_{m'}^{l'}, \quad (A5)$$

where  $\langle l, m; l', m' | \lambda, \lambda' \rangle$  is the corresponding Clebsch-Gordan coefficient. The interaction component can be expressed by applying the irreducible tensor coupling [75] as

$$H_{SO}^{int} = \frac{i\sqrt{6}}{2} [1 + \hat{P}(A, B)] \times \left[ \sum_{\alpha \in A} \sum_{j \in B} \frac{Z_{\alpha}}{r_{j\alpha}^3} \{[\mathbf{r}_{j\alpha} \otimes \mathbf{p}^1(j)]^1 \otimes \mathbf{s}^1(j)\}^0 - \sum_{j \in A} \sum_{k \in B} \left( \frac{1}{r_{jk}^3} \{[\mathbf{r}_{jk} \otimes \mathbf{p}^1(j)]^1 \otimes \mathbf{s}^1(j)\}^0 - 2\{[\mathbf{r}_{jk} \otimes \mathbf{p}^1(k)]^1 \otimes \mathbf{s}^1(j)\}^0 \right) \right]. \quad (A6)$$

To proceed further, we use the following coordinate transformation:

$$\mathbf{r}_{jk} = \mathbf{r}_j - \mathbf{r}_k = \mathbf{r}_j - (\mathbf{R} - \mathbf{r}'_k) = \mathbf{r}_j - \mathbf{r}'_k - \mathbf{R}, \quad (A7)$$

where  $\mathbf{R}$  is the distance between the monomers. Then, we apply the following identity [75] for  $r_1 < r_2$ :

$$\frac{r_{1\mu}}{r^3} = 4\pi \sum_{l=1}^{\infty} (-1)^l \sqrt{\frac{l}{3}} \frac{r_1^{l-1}}{r_2^{l+1}} [Y^{l-1}(\Omega_1) \otimes Y^l(\Omega_2)]_{\mu}^1, \quad (A8)$$

where  $\mathbf{r} = \mathbf{r}_1 - \mathbf{r}_2$ , and  $(r_1, \Omega_1)$  and  $(r_2, \Omega_2)$  are the spherical coordinates of vectors  $\mathbf{r}_1$  and  $\mathbf{r}_2$ , respectively. In the present case,  $\mathbf{r}_1 = \mathbf{r}_j - \mathbf{r}'_k$  and  $\mathbf{r}_2 = \mathbf{R}$ . Then, the formula for the translation of the regular solid harmonic  $R_m^l(\mathbf{r})$  can be used [75]:

$$|\mathbf{r}_j - \mathbf{r}'_k|^{l-1} Y_{\mu}^{l-1}(\Omega_{\mathbf{r}_j - \mathbf{r}'_k}) = \sqrt{\frac{2(l-1)+1}{4\pi}} R_{\mu}^{l-1}(\mathbf{r}_j - \mathbf{r}'_k), \quad (\text{A9})$$

$$R_{\mu}^{l-1}(\mathbf{r}_j - \mathbf{r}'_k) = \sum_{\lambda=0}^{l-1} \binom{2l-2}{2\lambda}^{1/2} \sum_{\omega=-\lambda}^{\lambda} R_{\omega}^{\lambda}(\mathbf{r}_j) R_{\mu-\omega}^{l-1-\lambda}(-\mathbf{r}'_k) \langle \lambda, \omega; l-1-\lambda, \mu-\omega | l-1, \mu \rangle, \quad (\text{A10})$$

$$R_{\mu}^{l-1}(\mathbf{r}_j - \mathbf{r}'_k) = \sum_{\lambda=0}^{l-1} \binom{2l-2}{2\lambda}^{1/2} [R^{\lambda}(\mathbf{r}_j) \otimes R^{l-1-\lambda}(-\mathbf{r}'_k)]_{\mu}^{l-1}. \quad (\text{A11})$$

Using all the above identities and recoupling the tensor operators in the spirit of Wormer [31] (i.e., in such a way that the operators acting on the coordinates of the monomers A and B are separated) the two-center multipole long-range expansion of the interaction component,  $H_{\text{SO}}^{\text{int}}$ , can be represented in the form

$$H_{\text{SO}}^{\text{int}} = \sum_{l_A=0}^{\infty} \sum_{l_B=0}^{\infty} \frac{i\sqrt{6}}{2 R^{l_A+l_B+2}} [1 + \hat{P}(\mathbf{A}, \mathbf{B}) (-1)^{l_A+l_B+1}] \left\{ \sum_{\lambda} \tau_{\lambda}^{l_A, l_B} [\mathbf{Q}^{l_B}(\mathbf{B}) \otimes \sum_{j \in \mathbf{A}} [\mathbf{R}^{l_A}(\vec{r}_j) \otimes [\mathbf{p}^l(\vec{r}_j) \otimes \mathbf{s}^l(j)]^1]_{\lambda}^{l_A+l_B+1}] \right. \\ \left. + 2 \sum_{\lambda, \lambda'} \gamma_{\lambda, \lambda'}^{l_A, l_B} \left[ \sum_{k \in \mathbf{B}} [\mathbf{R}^{l_B}(\vec{r}_k) \otimes \mathbf{p}^l(\vec{r}_k)]^{\lambda} \otimes \sum_{j \in \mathbf{A}} [\mathbf{R}^{l_A}(\vec{r}_j) \otimes \mathbf{s}^l(j)]^{\lambda'} \right]_{\lambda}^{l_A+l_B+1} \right\}. \quad (\text{A12})$$

The constants  $\tau_{\lambda}^{l_A, l_B}$  and  $\gamma_{\lambda, \lambda'}^{l_A, l_B}$  are fixed as

$$\tau_{\lambda}^{l_A, l_B} = (-1)^{l_B} \frac{(l_A + l_B + 1)^{1/2}}{3^{1/2}} (2l_A + 2l_B + 1) \binom{2l_A + 2l_B}{2l_A}^{1/2} (2\lambda + 1)^{1/2} \begin{Bmatrix} l_A & l_B & l_A + l_B \\ l_A + l_B + 1 & 1 & \lambda \end{Bmatrix}, \quad (\text{A13})$$

$$\gamma_{\lambda, \lambda'}^{l_A, l_B} = (-1)^{l_B} (l_A + l_B + 1)^{1/2} (2l_A + 2l_B + 1) (2\lambda + 1)^{1/2} (2\lambda' + 1)^{1/2} \binom{2l_A + 2l_B}{2l_A}^{1/2} \begin{Bmatrix} 1 & l_A & \lambda' \\ 1 & l_B & \lambda \\ 1 & l_A + l_B & l_A + l_B + 1 \end{Bmatrix}. \quad (\text{A14})$$

$\mathbf{Q}^l(\mathbf{A})$  denotes the operator of the multipole moment operator of rank  $l$  of the system A:

$$\mathbf{Q}_m^l(\mathbf{A}) = - \sum_{i \in \mathbf{A}} R_m^l(\vec{r}_i) + \sum_{\alpha \in \mathbf{A}} Z_{\alpha} R_m^l(\vec{r}_{\alpha}), \quad (\text{A15})$$

and  $\begin{Bmatrix} l_A & l_B & l_A + l_B \\ l_A + l_B + 1 & 1 & \lambda \end{Bmatrix}$  and  $\begin{Bmatrix} 1 & l_A & \lambda' \\ 1 & l_B & \lambda \\ 1 & l_A + l_B & l_A + l_B + 1 \end{Bmatrix}$  are Wigner 6j and 9j-symbols [75].

- 
- [1] H. Lefebvre-Brion and R. W. Field, *The Spectra and Dynamics of Diatomic Molecules* (Academic Press, San Diego, 2004).
- [2] S. N. Yurchenko, L. Lodi, J. Tennyson, and A. V. Stoliarov, *Comput. Phys. Commun.* **202**, 262 (2016).
- [3] H. Wang, P. Gould, and W. Stwalley, *Z. Physik D* **36**, 317 (1996).
- [4] Y. Takasu, Y. Fukushima, Y. Nakamura, and Y. Takahashi, *Phys. Rev. A* **96**, 023602 (2017).
- [5] K.-K. Ni, S. Ospelkaus, M. De Miranda, A. Pe'Er, B. Neyenhuis, J. Zirbel, S. Kotochigova, P. Julienne, D. Jin, and J. Ye, *Science* **322**, 231 (2008).
- [6] R. Krems, B. Friedrich, and W. C. Stwalley, *Cold Molecules: Theory, Experiment, Applications* (CRC Press, Boca Raton, 2009).
- [7] E. A. Pazyuk, A. V. Zaitsevskii, A. V. Stoliarov, M. Tamaniš, and R. Ferber, *Russ. Chem. Rev.* **84**, 1001 (2015).
- [8] J. Tennyson, L. Lodi, L. K. McKemmish, and S. N. Yurchenko, *J. Phys. B* **49**, 102001 (2016).
- [9] W. Stwalley, J. Banerjee, M. Bellos, R. Carollo, M. Recore, and M. Mastroianni, *J. Phys. Chem. A* **114**, 81 (2010).
- [10] J.-T. Kim, B. Kim, and W. C. Stwalley, *Analysis of the Alkali Metal Diatomic Spectra* (Morgan & Claypool Publishers, San Rafael, 2014).
- [11] M. Korek, G. Younes, and S. AL-Shawa, *J. Mol. Struct.: Theochem.* **899**, 25 (2009).
- [12] J. T. Kim, Y. Lee, and A. V. Stoliarov, *J. Mol. Spectrosc.* **256**, 57 (2009).
- [13] M. Tomza, W. Skomorowski, M. Musiał, R. González-Férez, C. P. Koch, and R. Moszynski, *Mol. Phys.* **111**, 1781 (2013).
- [14] Y. You, C.-L. Yang, Q.-Q. Zhang, M.-S. Wang, X.-G. Ma, and W.-W. Liu, *Phys. Chem. Chem. Phys.* **18**, 19838 (2016).
- [15] A. Zaitsevskii, N. S. Mosyagin, A. V. Stoliarov, and E. Eliav, *Phys. Rev. A* **96**, 022516 (2017).
- [16] E. A. Pazyuk, E. I. Revina, and A. V. Stoliarov, *Chem. Phys.* **462**, 51 (2015).

- [17] R. Vexiau, D. Borsalino, M. Lepers, A. Orbán, M. Aymar, O. Dulieu, and N. Bouloufa-Maafa, *Int. Rev. Phys. Chem.* **36**, 709 (2017).
- [18] E. A. Pazyuk, A. V. Stolyarov, A. Zaitsevskii, R. Ferber, P. Kowalczyk, and C. Teichteil, *Mol. Phys.* **96**, 955 (1999).
- [19] R. Ferber, E. A. Pazyuk, A. V. Stolyarov, A. Zaitsevskii, P. Kowalczyk, H. M. Chen, H. Wang, and W. C. Stwalley, *J. Chem. Phys.* **112**, 5740 (2000).
- [20] M. R. Manaa, *Int. J. Quantum Chem.* **75**, 693 (1999).
- [21] H. Harker, P. Crozet, A. J. Ross, K. Richter, J. Jones, C. Faust, J. Huennekens, A. V. Stolyarov, H. Salami, and T. Bergeman, *Phys. Rev. A* **92**, 012506 (2015).
- [22] M. Tamanis, R. Ferber, A. Zaitsevskii, E. A. Pazyuk, A. V. Stolyarov, H. M. Chen, J. B. Qi, H. Wang, and W. C. Stwalley, *J. Chem. Phys.* **117**, 7980 (2002).
- [23] O. Docenko, M. Tamanis, R. Ferber, E. A. Pazyuk, A. Zaitsevskii, A. V. Stolyarov, A. Pashov, H. Knockel, and E. Tiemann, *Phys. Rev. A* **75**, 042503 (2007).
- [24] K. Alps, A. Kruzins, M. Tamanis, R. Ferber, E. A. Pazyuk, and A. V. Stolyarov, *J. Chem. Phys.* **144**, 144310 (2016).
- [25] A. Adohi-Krou, W. Jastrzebski, P. Kowalczyk, A. V. Stolyarov, and A. J. Ross, *J. Mol. Spectrosc.* **250**, 27 (2008).
- [26] P. Kowalczyk, W. Jastrzebski, J. Szczepkowski, E. A. Pazyuk, and A. V. Stolyarov, *J. Chem. Phys.* **142**, 234308 (2015).
- [27] I. C. Stevenson, D. B. Blasing, A. Altaf, Y. P. Chen, and D. S. Elliott, *J. Chem. Phys.* **145**, 224301 (2016).
- [28] D. B. Blasing, I. C. Stevenson, J. Pérez-Ríos, D. S. Elliott, and Y. P. Chen, *Phys. Rev. A* **94**, 062504 (2016).
- [29] A. Dalgarno and W. Davison, *Adv. At. Mol. Phys.* **2**, 1 (1966).
- [30] A. D. Buckingham, in *Permanent and Induced Molecular Moments and LongRange Intermolecular Forces*, edited by J. O. Hirschfelder, Advances in Chemical Physics: Intermolecular Forces (John Wiley & Sons, 1967), Vol. 12, pp. 107–142.
- [31] P. E. S. Wormer, F. Mulder, and A. Van Der Avoird, *Int. J. Quantum Chem.* **11**, 959 (1977).
- [32] A. van der Avoird, P. E. S. Wormer, F. Mulder, and R. M. Berns, *Van der Waals Systems*, Topics in Current Chemistry, Vol. 93 (Springer, Berlin, Heidelberg, 1980), pp. 1–51.
- [33] B. Jeziorski, R. Moszynski, and K. Szalewicz, *Chem. Rev.* **94**, 1887 (1994).
- [34] M. Marinescu, H. R. Sadeghpour, and A. Dalgarno, *Phys. Rev. A* **49**, 982 (1994).
- [35] M. Marinescu and A. Dalgarno, *Phys. Rev. A* **52**, 311 (1995).
- [36] M. Marinescu and H. R. Sadeghpour, *Phys. Rev. A* **59**, 390 (1999).
- [37] G. A. Heijmen, R. Moszynski, P. E. S. Wormer, and A. van der Avoird, *Mol. Phys.* **89**, 81 (1996).
- [38] E. A. Pazyuk, E. I. Revina, and A. V. Stolyarov, *J. Quant. Spectrosc. Radiat. Transfer* **177**, 283 (2016); *Proceedings of the 18th Symposium on High Resolution Molecular Spectroscopy (HighRus'15)*, Tomsk, Russia.
- [39] E. Bormotova, S. Kozlov, E. Pazyuk, and A. Stolyarov, *Phys. Chem. Chem. Phys.* **20**, 1889 (2018).
- [40] B. Ji, C.-C. Tsai, and W. C. Stwalley, *Chem. Phys. Lett.* **236**, 242 (1995).
- [41] R. J. LeRoy, *J. Quant. Spectrosc. Radiat. Transf.* **186**, 158 (2017).
- [42] R. J. LeRoy, *J. Quant. Spectrosc. Radiat. Transf.* **186**, 167 (2017).
- [43] R. J. LeRoy, *J. Quant. Spectrosc. Radiat. Transf.* **186**, 179 (2017).
- [44] R. J. LeRoy, *J. Quant. Spectrosc. Radiat. Transf.* **186**, 197 (2017).
- [45] R. J. LeRoy and A. Pashov, *J. Quant. Spectrosc. Radiat. Transf.* **186**, 210 (2017).
- [46] R. J. LeRoy, W. J. Keogh, and M. S. Child, *J. Chem. Phys.* **89**, 4564 (1988).
- [47] B. Ji, C. Tsai, L. Li, T. Whang, A. M. Lyyra, H. Wang, J. T. Bahns, W. C. Stwalley, and R. J. LeRoy, *J. Chem. Phys.* **103**, 7240 (1995).
- [48] J. Y. Seto, R. J. LeRoy, J. Vergés, and C. Amiot, *J. Chem. Phys.* **113**, 3067 (2000).
- [49] Y. Huang and R. J. LeRoy, *J. Chem. Phys.* **119**, 7398 (2003).
- [50] R. J. LeRoy, *J. Mol. Spectrosc.* **228**, 92 (2004).
- [51] A. Adohi-Krou, F. Martin, A. J. Ross, C. Linton, and R. J. LeRoy, *J. Chem. Phys.* **121**, 6309 (2004).
- [52] H. Salami, A. J. Ross, P. Crozet, W. Jastrzebski, P. Kowalczyk, and R. J. LeRoy, *J. Chem. Phys.* **126**, 194313 (2007).
- [53] R. J. LeRoy, N. S. Dattani, J. A. Coxon, A. J. Ross, P. Crozet, and C. Linton, *J. Chem. Phys.* **131**, 204309 (2009).
- [54] N. S. Dattani and R. J. LeRoy, *J. Mol. Spectrosc.* **268**, 199 (2011).
- [55] V. V. Meshkov, A. V. Stolyarov, and R. J. LeRoy, *J. Chem. Phys.* **135**, 154108 (2011).
- [56] R. J. LeRoy and R. D. E. Henderson, *Mol. Phys.* **105**, 663 (2007).
- [57] R. Moszynski, G. Łach, M. Jaszuński, and B. Bussery-Honvault, *Phys. Rev. A* **68**, 052706 (2003).
- [58] B. Bussery-Honvault, J.-M. Launay, and R. Moszynski, *Phys. Rev. A* **72**, 012702 (2005).
- [59] O. Allard, S. Falke, A. Pashov, O. Dulieu, H. Knöckel, and E. Tiemann, *Eur. Phys. J. D* **35**, 483 (2005).
- [60] H.-J. Werner, P. J. Knowles, G. Knizia, F. R. Manby, M. Schütz *et al.*, MOLPRO, version 2010.1, a package of *ab initio* programs, 2010, <http://www.molpro.net>.
- [61] M. M. Hurley, L. F. Pacios, P. A. Christiansen, R. B. Ross, and W. C. Ermler, *J. Chem. Phys.* **84**, 6840 (1986).
- [62] H.-J. Werner and P. J. Knowles, *J. Chem. Phys.* **82**, 5053 (1985).
- [63] P. J. Knowles and H.-J. Werner, *Theor. Chim. Acta* **84**, 95 (1992).
- [64] W. Müller, J. Flesch, and W. Meyer, *J. Chem. Phys.* **80**, 3297 (1984).
- [65] P. Fuentealba, H. Preuss, H. Stoll, and L. Von Szentpály, *Chem. Phys. Lett.* **89**, 418 (1982).
- [66] J. Mitroy, M. S. Safronova, and C. W. Clark, *J. Phys. B: Atom. Mol. Phys.* **43**, 202001 (2010).
- [67] A. Kramida, Yu. Ralchenko, J. Reader, and NIST ASD Team, NIST Atomic Spectra Database (ver. 5.3), <http://physics.nist.gov/asd> (National Institute of Standards and Technology, Gaithersburg, MD, 2015).
- [68] H. Katō, *Bull. Chem. Soc. Jpn.* **66**, 3203 (1993).
- [69] H. A. Bethe and E. E. Salpeter, *Quantum Mechanics of One- and Two-Electron Atoms* (Springer-Verlag, Berlin/Göttingen/Heidelberg, 1957).

- [70] P. R. Fontana and W. J. Meath, *J. Math. Phys.* **9**, 1357 (1968).
- [71] W. J. Meath, *J. Chem. Phys.* **48**, 227 (1968).
- [72] J. O. Hirschfelder and W. J. Meath, in *The Nature of Intermolecular Forces*, edited by J. O. Hirschfelder, *Advances in Chemical Physics: Intermolecular Forces* (John Wiley & Sons, 1967), Vol. 12, pp. 3–106.
- [73] See Supplemental Material at <http://link.aps.org/supplemental/10.1103/PhysRevA.99.012507> for the *ab initio* calculated spin-orbit coupling functions of the LiNa, LiK, LiRb, NaK, NaRb, and KRb molecules in graphical and in pointwise formats.
- [74] S. V. Kozlov, E. A. Pazyuk, and A. V. Stolyarov, *Phys. Rev. A* **94**, 042510 (2016).
- [75] D. M. Brink and G. R. Satchler, *Angular Momentum* (Clarendon Press, Oxford, 1975).